



Journal Name

COMMUNICATION

Pollen-like ZIF-8 colloidosomes via emulsion templating and etching

Received 00th January 20xx,
Accepted 00th January 20xx

Lucia Lupica-Spagnolo^a Daniel J. Ward^a, John-Joseph Marie^a, Smaragda Lympieropoulou^a and Darren Bradshaw^{*a}

DOI: 10.1039/x0xx00000x

www.rsc.org/

Dedicated to the memory of Professor David E. Fenton

We report a one-pot emulsion-templating strategy for the preparation of ZIF-8 microcapsules both in the presence and absence of surfactants. Capsule diameter is tuneable in the range 1 – 10 μm , and they can be post-synthetically etched with excess imidazole to form hierarchical architectures resembling *Oleaceae* pollen grains.

Microencapsulation is an important technology for a number of applications that depend on the protection and on-demand release of active species.¹ Of the microcapsule compositions available, hybrid materials combining inorganic and organic components are particularly attractive due to their numerous assembly methods and ability to incorporate multiple functionalities.²

Microporous metal-organic frameworks (MOFs) composed of metal ions and organic linkers have many properties suitable for encapsulation, including high surface area, ordered porosity, tuneable structures and functionality and in some cases stimuli-responsive behaviours.³ MOFs also find application in similar areas to microcapsules (e.g. catalysis, separation, controlled delivery, theranostics)⁴, and there are an increasing number of strategies by which to configure MOF-based capsular structures⁵ especially those based on hard⁶ and soft⁷ templating, surface-energy driven processes⁸, spray-drying⁹ and interfacial synthesis.¹⁰ Non-spherical hollow MOF architectures can also be formed via MOF-on-MOF¹¹ or MOF-on-MOP (MOP = metal-organic polyhedral)¹² core-shell structures, followed by preferential etching of the cores based on differing stabilities or solubilities (wrt the MOF shells), permitting ready access to complex multi-shelled structures.

We recently reported the preparation of MOF-based capsules from Pickering emulsions where MOF-stabilised emulsion droplets could act as templates for the formation of

MOF-polymer composite capsules for pH-triggered cargo release¹³ and magnetic MOF capsules for the encapsulation of enzymes for size-selective recyclable biocatalysis.¹⁴ In both cases preformed MOF particles¹⁵ were used to stabilise the initial emulsion droplets, and the zeolitic-imidazolate framework ZIF-8 ($\text{Zn}(\text{Melm})_2$, where Melm = 2-methylimidazole)¹⁶, has proved particularly effective due to its appropriate surface wettability and aqueous stability.¹³ ZIF-8 is also a key synthetic target for capsule formation due to its compatibility with complex biological entities¹⁷, and further to the methods previously described^{6,8-10} hollow ZIF nanospheres have also been prepared via soft templating using interfacial synthesis around stabilised inverse emulsion droplets¹⁸ and micellar templates in aqueous solution.¹⁹ In addition to the formation of capsules with large internal cavities, the preparation of hierarchically porous ZIFs to increase mass diffusion through these otherwise microporous solids is also important for adsorption and catalysis applications.²⁰

In this contribution we show that free-standing ZIF-8 capsules (and those of the Co-analogue ZIF-67) can be prepared in a facile one-pot synthesis by simply adding the framework precursors to a suitably stable oil-in water emulsion without the need to pre-form the particles as in our earlier reports.^{13,14} This functions equally effectively with or without the use of surfactant stabilisers that provide a simple means to tune the capsule size. Further, the capsules can be post-synthetically etched by N-H acidic heterocycles to form hierarchical structures similar in appearance to pollen grains.

For the templating of ZIF-8 capsular structures we first prepared an oil-in-water (o/w) emulsion using 25 μL of dodecane as the internal phase initially with SPAN-80 (90 mg) as a stabiliser. The biphasic mixture was homogenised for 2 mins@11,500 rpm using a shear force instrument. To the emulsion was added 0.5 mL of a 0.2 M aqueous solution of $\text{Zn}(\text{NO}_3)_2$, which was left to stand in the fridge for 3 hrs, followed by 2 mL of a 3.4 M Melm aqueous solution (final Zn:Melm ratio = 1:70). The 1:70 ratio was selected as this is reported to rapidly form ZIF-8 in aqueous solution^{21a} which could provide

^aSchool of Chemistry, University of Southampton, Highfield Campus, Southampton SO17 1BJ, U. K. D.Bradshaw@soton.ac.uk

Electronic Supplementary Information (ESI) available: [details of any supplementary information available should be included here]. See DOI: 10.1039/x0xx00000x

additional stabilisation to the emulsion droplets, and lower ratios ($< 1:60$) are known to precipitate impurity phases.^{21b} After 24 hrs the white solid was isolated by centrifugation, washed with EtOH and dried at r.t. Powder X-Ray diffraction (PXRD) indicates that phase-pure sodalite (sod) ZIF-8 is formed under these conditions, and scanning electron microscopy (SEM) images reveal the presence of well-defined hollow capsular structures and an absence of free (bulk) ZIF-8 crystals (Figure 1a-c). The capsules are largely between 0.75 – 1.25 μm in diameter with a shell thickness of ~ 100 nm. The capsule external surfaces appear relatively smooth and are comprised of small aggregated ZIF-8 particles typically < 100 nm in size.

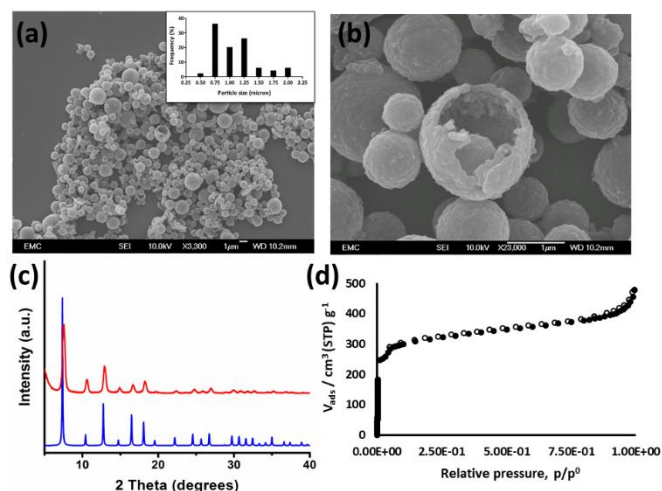


Figure 1. Characterisation data of emulsion-templated ZIF-8 colloidosomes formed in the presence of SPAN-80. (a), (b) SEM images (scale bar = $1\mu\text{m}$); the inset in (a) shows the size distribution histogram (50 capsules). (c) PXRD and (d) N_2 isotherm (77 K); closed circles, adsorption; open circles, desorption.

The nitrogen adsorption isotherm for the capsules is type I in nature with a slight increase in uptake at high relative pressure leading to a moderately hysteretic desorption profile (Figure 1d). This is consistent with textural mesoporosity arising from the interstices between the small ZIF-8 particles comprising the capsule shell walls, which is also suggested by BJH pore size distribution analysis (Figure S1). The capsules have an apparent Brunauer-Emmet-Teller (BET) surface area of $1180(1) \text{ m}^2/\text{g}$, and although generally modest for bulk ZIF-8 ($1500\text{--}1800 \text{ m}^2/\text{g}$) is comparable to hollow ZIF-8 microcrystals and nanospheres formed by solvent mediated overgrowth ($1276 \text{ m}^2/\text{g}$)²² and emulsion-templated interfacial synthesis ($984\text{--}1098 \text{ m}^2/\text{g}$)¹⁸, respectively. Thermogravimetric analysis (TGA) (Figure S2) reveals the capsules are thermally stable to 320°C , and the residual mass loss is indicative of the presence of $\sim 4 \text{ wt}\%$ SPAN-80 arising from the initial emulsion. This is consistent with the reduced surface area wrt bulk ZIF-8, and is further confirmed by SPAN-80 bands at 2900, 2800 and 1750 cm^{-1} in the FTIR spectrum of the capsules (Figure S3).

Although the synthesis of ZIF-8 under all of the conditions tested is highly consistent, formation of a stable homogeneous emulsion is clearly critical for capsule preparation. While we have not studied the dodecane-SPAN-80 emulsion *per se*, we

have investigated the influence of the amount of SPAN-80, the shear speed and duration on capsule formation.

If no shear force is applied to the biphasic dodecane-in-water system with SPAN-80 prior to addition of the ZIF-8 precursors then only very poorly defined colloidosomes or bulk ZIF-8 crystals are observed under a range of stirring conditions (Figure S4). The initial homogenisation of the emulsion is thus important for templating, and both shear force and length of time both have optimum values. When shear speeds of 9,500 or 14,500 rpm are applied similar results are obtained, and although SEM images of both samples reveal the presence of some hollow capsular structures, significant amounts of aggregated free ZIF-8 particles are also observed (Figure S5). Comparing these to the very well defined capsules obtained at a shear speed of 11,500 rpm, this suggests that the emulsions are insufficiently homogeneous when prepared in this way. Furthermore, time at the optimum shear speed is also important and while emulsions homogenised for 1 min do form predominantly capsular structures those emulsions prepared for 10 mins show a small number of large colloidosomes and many aggregated ZIF-8 particles (Figure S6). We therefore attribute the presence of free ZIF-8 crystals under the described synthetic conditions to emulsion inhomogeneity and/or instability.

Well-defined ZIF-8 colloidosomes are also successfully prepared when the amount of the SPAN-80 stabiliser is reduced (Figure S7), and most notably are still formed even in its absence (Figure 2a,b). Stable surfactant-free dodecane-in-water emulsions are known²³, and this is the first time such a system has been applied to the templating of MOF-based capsular structures: a previously reported one-pot synthesis of M-soc-MOF ($M = \text{Fe}, \text{Ga}$) colloidosomes employs a mixture of non-ionic surfactants⁷, and emulsion templated ZIF-8 is formed at a PVP (polyvinylpyrrolidone) stabilised interface.¹⁸

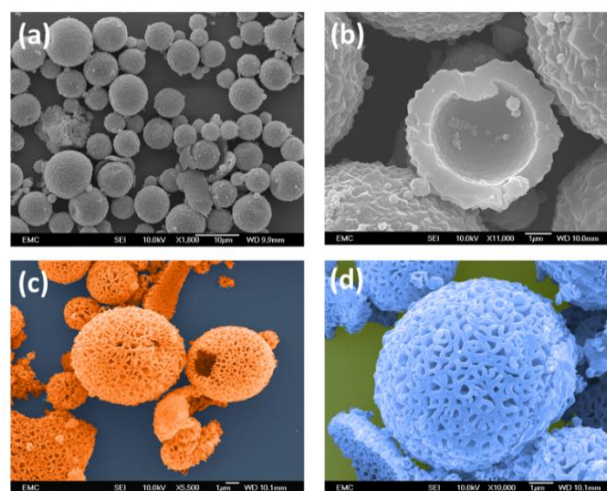


Figure 2. (a) and (b) SEM images of ZIF-8 colloidosomes formed using a surfactant free dodecane-water emulsion template, scale bars $10\mu\text{m}$ and $1\mu\text{m}$, respectively. (c) and (d) false coloured SEM images highlighting the hierarchical hollow structures formed when the colloidosomes are etched using an aqueous imidazole solution, scale bars both $1\mu\text{m}$.

In this case the ZIF-8 precursors are added sequentially and immediately following emulsification, and it is likely that the

rapid precipitation of the framework under these conditions provides instantaneous Pickering-type stabilisation to the emulsion droplets which then act as a substrate for ZIF-8 shell growth.¹⁴ This means that the dodecane-water emulsion only has to be stable for a relatively short time, suggesting other surfactant-free emulsions could be employed in a similar way.

SEM images of capsules formed from a surfactant-free emulsion using either 25 or 50 μL of dodecane as the internal phase have an average diameter of 5 – 10 μm (see also Figure S8) in both cases, and are thus larger than those formed in the presence of SPAN-80 ($\sim 1\mu\text{m}$) at similar volumes of added dodecane. Further the aggregated crystals which comprise the shell wall are larger than those observed in the presence of SPAN-80 and the capsule walls are generally thicker at 0.5 μm (Figure 2a,b). We note that the addition of SPAN-80 to bulk ZIF-8 syntheses does have an influence on particle size working as an effective additive to downsize the crystals to the nanoscale (Figure S9), and as previously reported for mixed SPAN-80/TWEEN surfactant systems.²⁴ This is consistent with the observations here, where addition of SPAN-80 to the emulsions reduces the droplet size through modification of interfacial tension²⁵ and the size of the crystals which comprise the shell resulting in smaller smoother capsules (Figure S10).

The surfactant free capsules are also sod-ZIF-8 as determined by PXRD, FTIR and TGA (Figure S11-S13). The nitrogen adsorption isotherm is type I in nature (Figure S14) and the capsules have a BET surface area of 1627(1) m^2/g consistent with the absence of SPAN-80 during synthesis and reduced textural mesoporosity between the larger crystals in the shell wall. By replacing the Zn(II) salt with $\text{Co}(\text{NO}_3)_2$, ZIF-67 colloidosomes are also readily accessible under both the surfactant and surfactant-free emulsion templated conditions with comparable results as shown in Figures S15 and S16.

Interestingly, the ZIF-8 colloidosomes can be chemically etched using an excess of imidazole (Im) in water. The resulting hollow architectures have a hierarchical structure, with intricate surface features that appear to penetrate through to the capsule interior (Figure 2c,d). The structure of the etched capsules are reminiscent of *Oleaceae* pollen grains (Figure S17) which display surface patterns on a similar length scale. We note the etching is independent of whether the capsules were prepared in the presence of SPAN-80 or not.

The observed features begin to appear at relatively short etching times (< 20 mins) with full preservation of the ZIF-8 lattice; however, when samples are left in the etching solution for several hrs a second phase is present in both the SEM images and PXRD data (Figure 3). This corresponds to a dense **zni** topology that has previously been reported for pure $\text{Zn}(\text{Im})_2$ (e.g. ZIF-61) and some mixed linker $\text{Zn}(\text{MeIm})(\text{Im})$ frameworks.²⁶ Its co-existence with the colloidosomes is clear evidence that the ZIF-8 components are leached into the etching solution, and ^1H NMR of digested samples that have been etched to completion (i.e. no observable colloidosomes) for 24 hrs are pure **zni** and contain 95% Im.

Etching of the ZIF-67 colloidosomes under the same conditions yields similar pollen-like architectures (Figure S18), but these are amorphous in nature indicating a breakdown of

the ordered sodalite topology (Figure S19). We attribute this to the differing stabilities of ZIF-8 and ZIF-67, which have previously been exploited to generate hollow ZIF-8 materials from ZIF-67@ZIF-8 core-shell structures by selective and preferential etching of the ZIF-67 cores.²⁷ We note that a similar transformation to an amorphous phase is also observed for bulk ZIF-67 under the same conditions (Figure S20), despite a recent report of the successful solvent-assisted linker exchange of ZIF-67 with a N-H acidic triazole species: the SALE was carried out in DMF or EtOH with retention of the sodalite structure.²⁸ The formation of the observed amorphous phase thus appears to be limited to when water is employed as the solvent, likely as a result of increased acidity under purely aqueous conditions.

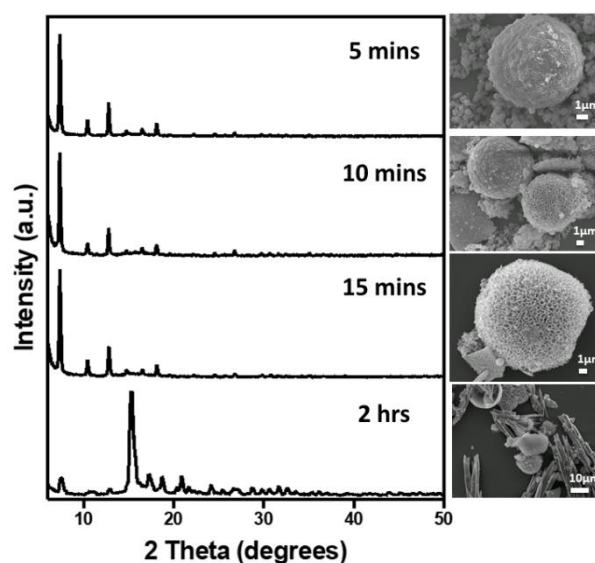


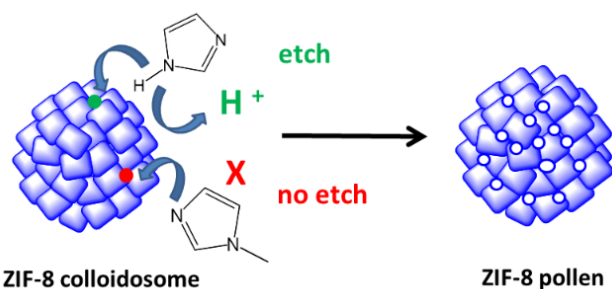
Figure 3. PXRD data and SEM images corresponding to different etching times of the ZIF-8 colloidosomes in aqueous imidazole. At longer etching times (e.g. 2 hrs) the presence of a dense **zni** phase is clearly evident which coexists with the etched sod-ZIF-8 colloidosomes.

In order to investigate whether Im has a specific role in the observed etching we replaced this with 1-Melm (1-methylimidazole) in the aqueous etching solution. Following 2 hrs of exposure, the colloidosomes showed no sign of being etched by 1-Melm (Figure S21), which suggests that the N-H acidity of Im may be important to the process. The role of protons is further confirmed by similar etching of the colloidosomes using pyrazole but not pyrimidine over relatively short time periods (Figure S22). PXRD and SEM images of the pyrazole etched capsules also reveal the presence of a second as yet unidentified phase (c.f. appearance of the **zni** structure when etched with Im), whereas with pyrimidine the sod-ZIF-8 structure is fully retained (Figure S23).

Post-synthetic acid etching of ZIF-8 has been previously reported using xylenol orange (XO) for facet-selective etching²⁹ and phenolic acids (PAs) to leave macroscopic cavities within the parent crystals via a surface-functionalized assisted etching strategy.³⁰ In both cases etching occurs due to released protons breaking down the framework coordination interactions. The acid etchants also play secondary roles: XO acts as a chelating agent to sequester and solubilise the liberated metal ions to

prevent unwanted side-reactions, and the PAs switch ZIF-8 surface properties to facilitate proton mobility within the framework and protect the external surface localising etching within the crystal interiors.

With this in mind we propose a proton-based etching mechanism (Scheme 1) for the ZIF-8 colloidosomes which is initially promoted in the interstices/grain boundaries between particles in the capsule shell wall where the Im potentially concentrates. Here a proton exchange occurs between the Im and the more basic 2-Melm framework linkers, facilitated by the aqueous solvent²² and the ability of Im to act as a buffer at the ~1M concentration employed. The more hydrophilic nature of Im over Melm may further promote etching in the regions where this is concentrated, breaking down the framework linkages and releasing the components into the etchant solution where the Zn(II) ions in particular combine with the excess Im to form the observed **zni** phase as the etching proceeds.



Scheme 1. Illustration of the proposed etching process of ZIF-8 colloidosomes by N-H acidic N-heterocyclic species in water.

In summary we report the efficient one-pot emulsion-templating of free-standing ZIF-8 colloidosomes both in the presence and absence of surfactants, which permits a level of size-control over the resulting capsules. The colloidosomes can be post-synthetically etched in a controlled way by N-H acidic heterocyclic species to form intricate hierarchical structures that resemble pollen grains. It is anticipated that the ZIF-8 capsules could find application across a range of sectors including healthcare, where the etching process could be exploited for controlled release or sensing in response to external changes in pH or the presence of biomarkers based on N-H acidic heterocycles.

We thank the European Research Council for funding (BIOMOF-258613), the EPSRC for the award of a student vacation bursary to DJW and India Willimott for experimental assistance.

Conflicts of Interest

There are no conflicts to declare.

Notes and references

- 1 *Microencapsulation – Methods and Industrial Applications*, ed. S. Benita, CRC press, Taylor & Francis Group, 2006.
- 2 J. Shi, Y. Jiang, X. Wang, H. Wu, D. Yang, F. Pan, Y. Su and Z. Jiang, *Chem. Soc. Rev.*, 2014, **43**, 5192.
- 3 (a) H. Furukawa, K. E. Cordova, M. O’Keeffe and O. M. Yaghi, *Science*, 2013, **341**, 1230444; (b) C. Janiak and J. K. Vieth, *New J. Chem.*, 2010, **34**, 2366; (c) G. Férey, *Chem. Soc. Rev.*, 2008, **37**, 191; (d) F.-X. Coudert, *Chem. Mater.*, 2015, **27**, 1905.
- 4 MOF special issues, *Chem. Soc. Rev.*, 2009, **38**, 1201–1508; *Chem. Soc. Rev.*, 2014, **43**, 5403–6176.
- 5 H. Kim and M. S. Lah, *Dalton Trans.*, 2017, **46**, 6146.
- 6 H. J. Lee, W. Cho and M. Oh, *Chem. Commun.*, 2012, **48**, 221.
- 7 M. L. Pang, A. J. Cairns, Y. L. Liu, Y. Belmabkhout, H. C. Zeng and M. Eddaoudi, *J. Am. Chem. Soc.*, 2013, **135**, 10234.
- 8 Z. Zhang, Y. Chen, X. Xu, J. Zhang, G. Xiang, W. He and X. Wang, *Angew. Chem., Int. Ed.*, 2014, **53**, 429.
- 9 A. Carne-Sanchez, I. Imaz, M. Cano-Sarabia and D. Maspocho, *Nat. Chem.*, 2013, **5**, 203.
- 10 R. Ameloot, F. Vermoortele, W. Vanhove, M. B. J. Roeyfaers, B. F. Sels and D. E. De Vos, *Nat. Chem.*, 2011, **3**, 382.
- 11 W. Liu, J. Huang, Q. Yang, S. Wang, X. Sun, W. Zhang, J. Liu and F. Huo, *Angew. Chem., Int. Ed.*, 2017, **56**, 5512.
- 12 J. Li, J. H. Kwak and W. Choe, *Nat. Comm.*, 2017, **8**, 14070.
- 13 J. Huo, M. Marcello, A. Garai and D. Bradshaw, *Adv. Mater.*, 2013, **25**, 2717.
- 14 J. Huo, J. Aguilera-Sigalat, S. El-Hankari and D. Bradshaw, *Chem. Sci.*, 2015, **6**, 1938.
- 15 B. Xiao, Q. Yuan and R. A. Williams, *Chem. Commun.*, 2013, **49**, 8208.
- 16 (a) K. S. Park, Z. Ni, A. P. Cote, J. Y. Choi, R. Huang, F. J. Uribe-Romo, H. K. Chae, M. O’Keeffe and O. M. Yaghi, *Proc Natl Acad Sci U S A*, 2006, **103**, 10186; (b) B. Chen, Z. Yang, Y. Zhu and Y. Xia, *J. Mater. Chem. A*, 2014, **2**, 16811.
- 17 R. Ricco, W. Liang, S. Li, J. J. Gassensmith, F. Caruso, C. Doonan and P. Falcaro, *ACS Nano*, 2018, **12**, 13.
- 18 Y. Yang, F. Wang, Q. Yang, Y. Hu, H. Yan, Y.-Z. Chen, H. Liu, G. Zhang, J. Lu, H.-L. Jiang and H. Xu, *ACS Appl. Mater. Interfaces*, 2014, **6**, 18163.
- 19 Y. C. Tan and H. C. Zeng, *Chem. Commun.*, 2016, **52**, 11591.
- 20 (a) H. N. Abdelhamid and X. Zou, *Green Chem.*, 2018, **20**, 1074; (b) H. N. Abdelhamid, Z. Huang, A. M. El-Zohry, H. Zheng and X. Zou, *Inorg. Chem.*, 2017, **56**, 9139; (c) K. Shen, L. Zhang, X. Chen, L. Liu, D. Zhang, Y. Han, J. Chen, J. Long, R. Luque, Y. Li and B. Chen, *Science*, 2018, **359**, 206.
- 21 (a) Y. Pan, Y. Liu, G. Zeng, L. Zhao and Z. Lai, *Chem. Commun.*, 2011, **47**, 2071; (b) K. Kida, M. Okita, K. Fujita, S. Tanaka and Y. Miyake, *CrystEngComm*, 2013, **15**, 1794.
- 22 L.-Y. Chou, P. Hu, J. Zhuang, J. V. Morabito, K. C. Ng, Y.-C. Cao, S.-C. Wang, F.-K. Shieh, C.-H. Kuo and C.-K. Tsung, *Nanoscale*, 2015, **7**, 19408.
- 23 T. Sakai, *Current Opinion in Colloid and Interface Science*, 2008, **13**, 228.
- 24 X. Fan, W. Wang, W. Li, J. Zhou, B. Wang, J. Zheng and X. Li, *ACS Appl. Mater. Interfaces*, 2014, **6**, 14994.
- 25 E. Santini, L. Liggieri, L. Sacca, D. Clause and F. Ravera, *Colloids and Surfaces A: Physico. Eng. Aspects*, 2007, **309**, 270.
- 26 (a) R. Banerjee, A. Phan, B. Wang, C. Knobler, H. Furukawa, M. O’Keeffe and O. M. Yaghi, *Science*, 2008, **319**, 939; (b) D. W. Lewis, A. R. Ruiz-Salvador, A. Gómez, L. M. Rodríguez-Albelo, F.-X. Coudert, B. Slater, A. K. Cheetham and C. Mellot-Draznieks, *CrystEngComm*, 2009, **11**, 2272.
- 27 (a) C. Rosler, A. Aijaz, S. Turner, M. Filippousi, A. Shahabi, W. Xia, G. Van Tendeloo, M. Muler and R. A. Fischer, *Chem. Eur. J.*, 2016, **22**, 3304; (b) J. Yang, F. Zhang, H. Lu, X. Hong, H. Jiang, Y. Wu and Y. Li, *Angew. Chem. Int. Ed.*, 2015, **54**, 10889.
- 28 M. Erkartel, U. Erkilic, B. Tam, H. Usta, O. Yazaydin, J. T. Hupp, O. K. Farha and U. Sen, *Chem. Commun.*, 2017, **53**, 2028.
- 29 C. Avci, J. Arinez-Soriano, A. Carne-Sanchez, V. Guillerm, C. Carbonell, I. Imaz and D. Maspocho, *Angew. Chem. Int. Ed.*, 2015, **54**, 14417.
- 30 M. Hu, Y. Ju, K. Liang, T. Suma, J. Cui and F. Caruso, *Adv. Funct. Mater.*, 2016, **26**, 5827.